buildings

MDPI

Article

Experimental Behavior of Confined Masonry Walls Rehabilitated with Reinforced Mortar Jacketing Subjected to Cyclic Loading

Cyprien Lubin [1,*], Hector Guerrero [1,*], Sergio M. Alcocer [1] and Oscar Lopez Batiz [2]

[1] Institute of Engineering, UNAM, Mexico City 04510, Mexico; salcocerm@iingen.unam.mx
[2] National Center for Disaster Prevention, Mexico City 04360, Mexico; olb@cenapred.unam.mx
* Correspondence: clubin@iingen.unam.mx (C.L.); hguerrerob@iingen.unam.mx (H.G.)

Abstract: Results of an experimental program of 13 confined masonry walls rehabilitated with different techniques are presented. All specimens were built to full-scale with an aspect ratio (height to length) of 1. Vertical confining elements of one wall were built with 6.4 mm diameter welded wire reinforcing cages. Before rehabilitation, 11 of the 13 walls were initially tested to induce repairable damage; the other 2 were strengthened in an undamaged state. During testing, walls were subjected to a constant vertical load. Initially, damaged walls were rehabilitated using various techniques, such as jacketing made of mortar and welded wire mesh and synthetic or steel fibers. One initially damaged wall was rehabilitated with premixed mortar and fiberglass mesh. After rehabilitation, specimens were tested for failure. The experimental program is discussed, including materials characterization and main test results. Recommendations to practicing engineers involved in rehabilitating earthquake-damaged masonry structures are presented. It was found that the original capacity of the walls, in terms of strength, stiffness, and deformation, was increased considerably using the studied techniques. It is concluded that the techniques evaluated in this project are adequate for the seismic rehabilitation of masonry structures.

Keywords: confined masonry walls; seismic rehabilitation; experimental; welded-wire mesh; wall jacketing

check for updates

Citation: Lubin, C.; Guerrero, H.; Alcocer, S.M.; Lopez Batiz, O. Experimental Behavior of Confined Masonry Walls Rehabilitated with Reinforced Mortar Jacketing Subjected to Cyclic Loading. *Buildings* **2023**, *13*, 1314. https://doi.org/10.3390/buildings13051314

Academic Editor: Bartolomeo Pantò

Received: 15 April 2023
Revised: 14 May 2023
Accepted: 16 May 2023
Published: 18 May 2023

1. Introduction

In many regions worldwide, masonry walls are the most widely used structural elements to resist vertical and horizontal forces in residential buildings, either in single-family or multi-family buildings, due to their low cost and simplified construction process [1]. Masonry walls are considered confined when the panel is first constructed, and reinforced concrete (RC) vertical and horizontal ties are subsequently cast around its perimeter. These elements increase the inelastic deformation capacity of the wall and its strength to lateral forces. Generally, they are placed at corners and intersections, at the edges of doors and windows, or where seismic forces are concentrated. The confined masonry design practice is already included in construction regulations of different countries and regions worldwide [2].

Numerous experimental studies have been carried out to evaluate the response of masonry walls to lateral loads. For example, Varela et al. [3] observed through experimental studies that flexural failure, more common in thin walls, was associated with concrete crushing at the vertical confining elements, followed by vertical and diagonal cracks on the masonry panel. Leon et al. [4], based on experimental studies of confined masonry under compressive loads, reported that the concrete of the vertical ties takes up to 75 percent of the compressive loads, while the masonry panel receives the remaining 25 percent.

Although several studies about the behavior of masonry and its failure mechanisms worldwide are available, highly vulnerable masonry buildings continue to be observed, especially in regions close to seismic sources. For this reason, it is vitally important to develop rehabilitation techniques that are easy to implement at low cost to increase our communities' seismic resiliency.

Earthquakes are one of the major natural disasters that cause huge social impacts and property losses [5]. Given the damage observed in past earthquakes in masonry buildings, various rehabilitation and strengthening techniques, such as external sub-structure retrofitting, steel jacketing, or reinforced mortar jacketing, have been proposed and studied in recent decades to improve their behavior [5,6]. Among these techniques are: ferrocement and polymers reinforced with glass fibers [7,8], horizontal reinforcing steel bars and wires placed in mortar joints [9], welded wire mesh-reinforced mortar [10–14], carbon fiber mesh-reinforced mortar [15], basalt fiber mesh-reinforced mortar [16], textile-reinforced mortar [17] and fiber-reinforced mortar [18–20].

Regarding rehabilitation with ferrocement and fiberglass-reinforced polymer, El-Diasity [7] conducted an experimental study of 10 confined masonry walls made of clay brick units. Walls were built to a scale of 0.8 and tested under in-plane cyclic loading. After inducing damage, some walls were rehabilitated with ferrocement and others with fiberglass-reinforced polymer. Similar behavior with both rehabilitation techniques was observed in the tested walls. Lateral strength was found to increase between 25 and 32 percent, while the increase in the deformation capacity was less significant.

Cruz and Pérez [9] tested eight confined masonry walls built to full-scale with horizontal reinforcing steel bars embedded in the mortar joints. Specimens were tested under reversed cyclic lateral loads and constant vertical stress. Results showed that the horizontal reinforcing steel increased the lateral strength and decreased stiffness degradation of the walls but reduced lateral ductility. These tests concluded that although horizontal reinforcing steel at the joints is adequate for new walls, it may not be feasible to rehabilitate existing walls damaged by seismic actions.

Shermi [11] studied the behavior of 24 masonry walls subjected to out-of-plane loading. Eighteen walls were strengthened with wire mesh-reinforced mortar before being tested, while the other six were tested in their original state. For the construction of the specimens, two types of joint mortar commonly used in practice in India were employed: one with high resistance (cement: sand with 1:4 dosage) and the other with low resistance (cement: sand with 1:6 dosage). Cement: sand mortar was used for the rehabilitated specimens with 1:3 dosages and reinforced with welded wire mesh with various wire spacing (25 mm, 38 mm, and 50 mm, respectively). Failure modes and behavior of masonry walls were studied regarding strength, stiffness, and ductility. It was observed that the out-of-plane flexural strength of the strengthened walls was up to 20 times higher than that of the original walls, while their ductility increased by three times.

Alcocer et al. [12] and Alcocer [13] assessed experimentally the technical feasibility of jacketing (concrete mortar cover reinforced with steel welded wire meshes) as a rehabilitation technique for confined masonry walls. Four full-scale specimens were rehabilitated and tested under reversed cyclic lateral loads; variables studied included the level of damage, type, and size of specimens (two-story three-dimensional and one-story two-dimensional), the wire diameter of the mesh and the types of anchors used to fix the meshes to the masonry walls. Results indicated that jacketing of confined masonry walls with steel meshes and a mortar cover is an effective technique for improving the earthquake-resistant capacity.

The Mexican Society of Structural Engineering [14] has reported that masonry structures' most reliable, efficient, and economical rehabilitation technique is placing welded steel mesh anchored adequately to the walls covered with mortar. According to this report, using this technique, the original strength, stiffness, and deformation capacity increased by 50, 20, and 100 percent, respectively.

Gattesco [8] studied a rehabilitation technique applying a mortar cover on both wall faces reinforced with glass fiber-reinforced polymer (GFRP) meshes. Four-point bending tests of three full-scale masonry walls, 1 m wide and 3 m high, built with three different masonry units, were conducted. Results for the original walls and the rehabilitated ones were compared. It was observed that the out-of-plane flexural strength capacity of the rehabilitated walls was up to five times greater than that of the original walls.

Can [15] tested 36 wall panels, 900 × 900 × 200 mm, using three masonry units (hollow masonry bricks, blend bricks, and autoclaved aerated concrete bricks). Panels were reinforced with carbon fibers using three different methods: (1) with unidirectional carbon fiber over the entire wall surface, (2) with carbon fiber in an orthogonal grid pattern over both faces of the wall, and (3) with two carbon fiber strips along the diagonals of the wall covering the same surface as the former method. Results showed that all the strengthening methods were adequate since they increased the lateral load strength, displacement capacity, and energy dissipation. No notable differences were observed between the different strengthening methods, so the diagonal method was considered the most efficient because it used less material than the other methods.

D'Ambra [16] proposed rehabilitating masonry walls using a composite basalt grid with an inorganic matrix (FRCM). Experimental tests were conducted on two full-scale clay brick walls subjected to out-of-plane loads. One of the two specimens was initially damaged before rehabilitation, while the other was strengthened in its undamaged state. It was observed that the peak load capacity of walls strengthened with a basalt fiber grid almost doubled that of walls initially damaged before rehabilitation. Furthermore, the rehabilitation technique was able to prevent a brittle failure. It was also reported that shear sliding was the dominant failure mechanism of the strengthened walls.

Yacila [19] conducted an experimental study of confined masonry walls retrofitted with Steel Reinforced Grout subjected to lateral cyclic in-plane loads. The experiments involved repairing three previously damaged, full-scale walls using five horizontal strips of mortar reinforced with steel fibers. The mortar strips had a width of 100 mm and a thickness of 10 mm. A galvanized steel fiber mesh (with a thickness of 0.084 mm) was embedded within each strip. The results showed an increase of up to 100 percent in the inelastic deformation capacity, a greater dissipation of energy, and a greater initial degradation of lateral stiffness of the rehabilitated walls than the original ones.

Deng and Yang [21] built and tested five confined masonry walls and four unreinforced specimens made of autoclaved aerated concrete (AAC) blocks. Two walls, one confined and one unreinforced, served as benchmark specimens, while the others were rehabilitated with different configurations of reinforced-concrete cover with high ductility synthetic fibers. The specimens' damage evolution, failure modes, and force-displacement curves were analyzed. From these results, the response of the walls was evaluated considering their capacity to resist lateral force, their ductility, their energy dissipation capacity, and their degradation of energy. It was observed that the rehabilitation with synthetic fibers could increase the shear strength and energy dissipation of unreinforced masonry walls. In contrast, the increase in the inelastic deformation capacity was negligible.

The literature review observed that some experimental studies used different rehabilitation techniques for confined and unreinforced masonry walls. Reinforced mortar with different materials, such as wire mesh, stands out among these techniques. Its popularity is perhaps due to its low cost and simplicity of design and construction. The results of these experiments provide valuable data on the adequacy of these techniques used on masonry walls. Although there have been some experiments, they are still scarce since there are many variables that must be studied, such as the wire mesh diameter, the mesh-to-wall anchorage type, the mortar strength, the number of wall sides to rehabilitate, the steel reinforcement in the concrete confining elements, among others. The effects of these variables on the deformation and load capacity of masonry walls must be further studied to understand better their contribution to the structural response of seismically rehabilitated structures.

This paper presents the results of an experimental program consisting of tests of 13 full-scale confined masonry walls rehabilitated using different techniques and subjected to in-plane cyclic lateral loading. The results aimed to contribute to a better understanding of the effectiveness of rehabilitating damaged masonry walls and improving our communities' seismic resiliency. Diverse effects were assessed within the rehabilitation process, such as the type of mortar (hand-mixed or premixed), wire mesh size, synthetic fibers, steel fibers, or the combination of wire mesh and fibers. The number of wall sides to rehabilitate and the type of anchorage from the mesh to the masonry were also varied. In addition, one of the walls was built with welded-wire reinforcing cages in the confining elements and later rehabilitated with wire mesh-reinforced mortar. A discussion of these effects on the load capacity, lateral deformation, stiffness degradation, damping factor, and ductility is presented. Conclusions applicable to rehabilitating damaged structures after earthquakes are offered at the end.

2. Experimental Program

2.1. Tested Specimens

Thirteen confined masonry walls with a height and width of 2.50 m and a thickness of 120 mm were built to full scale and tested in the Large-Scale Structures Laboratory of Mexico's National Center for Disaster Prevention, CENAPRED [22]. They were built using hand-made solid clay bricks with nominal dimensions of 60 $\times$ 120 $\times$ 240 mm (thickness $\times$ height $\times$ length).

The confining elements of masonry walls consisted of a 120 $\times$ 300 mm bond beam (horizontal element) and two 120 $\times$ 200 mm tie-columns (vertical elements). The horizontal element was reinforced with four no. 3 (9.5 mm diameter) bars. Vertical elements had the following longitudinal reinforcing steel: specimens M1 to M4 had four no. 4 (13 mm diameter) bars; specimens M5 to M12 had eight no. 4 (13 mm diameter) bars; specimen M13 was built with welded wire steel cages. The horizontal bond beam of the 13 specimens was cast monolithically with a 100 mm-thick and 450 mm-wide reinforced concrete slab. The steel of the longitudinal reinforcement of tie columns and bond beams had a nominal yield strength of 420 MPa. The transverse reinforcement consisted of no. 2 (6.25 mm diameter) stirrups, spaced at 150 mm, made of steel with a yield strength of 230 MPa. The steel reinforcement of specimen M13 had a nominal yield strength of 500 MPa.

The characteristics of the 13 specimens, denoted as M1 to M13, are presented in Table 1. Figure 1 is added to facilitate the identification of specimen features. Note that specimens M3 and M4 were not initially damaged, while the others were damaged to assess the effect of initial damage on the performance of the rehabilitation technique. Specimens M1 to M4 were rehabilitated on both faces, while the others were rehabilitated only on one face. The mortar was hand-mixed or premixed. The hand-mixed mortar was made with Portland cement and sand, using a volumetric ratio of 1:3, respectively. The premixed mortar was Sika Monotop-722 Mur [23], with nominal compressive strength of 22 MPa. Welded wire meshes (WWM) had wired diameters of 3.4 mm (10-cal) or 4.2 mm (8-cal). Other specimens were jacketed with steel fibers (MF), synthetic fibers (SF), or glass fiber meshes (GFM). Specimens M9 and M10 were rehabilitated using buckling-restrained braces (BRBs). The anchorage of the WWM to the masonry was made of steel nails or wire spaced at 450 mm. Specimens M11 and M12 were rehabilitated by combining two techniques: (1) steel WWM with synthetic fibers or (2) steel WWM with steel fibers. Synthetic fibers were Sika Fiber Force PP-48 [24], and steel fibers were Sika Fiber Xorex [25]. Vertical tie-columns of specimen M13 had longitudinal and transverse reinforcement made of steel welded wire cages. The wire had a diameter of 3.4 mm. Four wires were provided in the longitudinal direction, while the transverse reinforcement consisted of stirrups spaced at 150 mm. This reinforcement was used on specimen M13 because it is popular in engineered and non-engineered constructions in several countries worldwide.

Table 1. Characteristics of the tested specimens.

	Damage		F *	Rehab. Mortar	Strengthening Method	Anchorage
Spec.	In.D	Rehab.		25 mm@side		
M1	Yes	Yes	Both	cement-sand 1:3	WWM 10-cal	Steel nails@450 mm
M2	Yes	Yes	Both	cement-sand 1:3	WWM 8-cal	Steel nails@450 mm
M3	No	Yes	Both	cement-sand 1:3	WWM 8-cal	Steel nails@450 mm
M4	No	Yes	Both	cement-sand 1:3	WWM 10-cal	Steel nails@450 mm
M5	Yes	Yes	One	cement-sand 1:3	MF	N/A
M6	Yes	Yes	One	cement-sand 1:3	WWM 8-cal	Wire rod@450 mm
M7	Yes	Yes	One	cement-sand 1:3	SF	N/A
M8	Yes	Yes	One	Premixed	FGM	N/A
M9	Yes	Yes	N/A	N/A	BRB	N/A
M10	Yes	Yes	N/A	N/A	BRB	N/A
M11 **	Yes	Yes	One	cement-sand 1:3	WWM 10-cal and SF	Steel nails@450 mm
M12 **	Yes	Yes	One	cement-sand 1:3	WWM 10-cal and MF	Steel nails@450 mm
M13	Yes	Yes	One	cement-sand 1:3	WM 10-cal	Steel nails@450 mm

* F = Faces of the wall rehabilitated; In.D = Initially damaged; RE = Rehabilitated; WWM = Welded Wire Mesh; N/A = not applicable; MF = Metallic (Steel) Fiber; SF = Synthetic Fiber; FGM = Fiber Glass Mesh. ** Specimens M11 and M12 were originally covered with a 25 mm layer of premixed mortar StoneCrete [26].

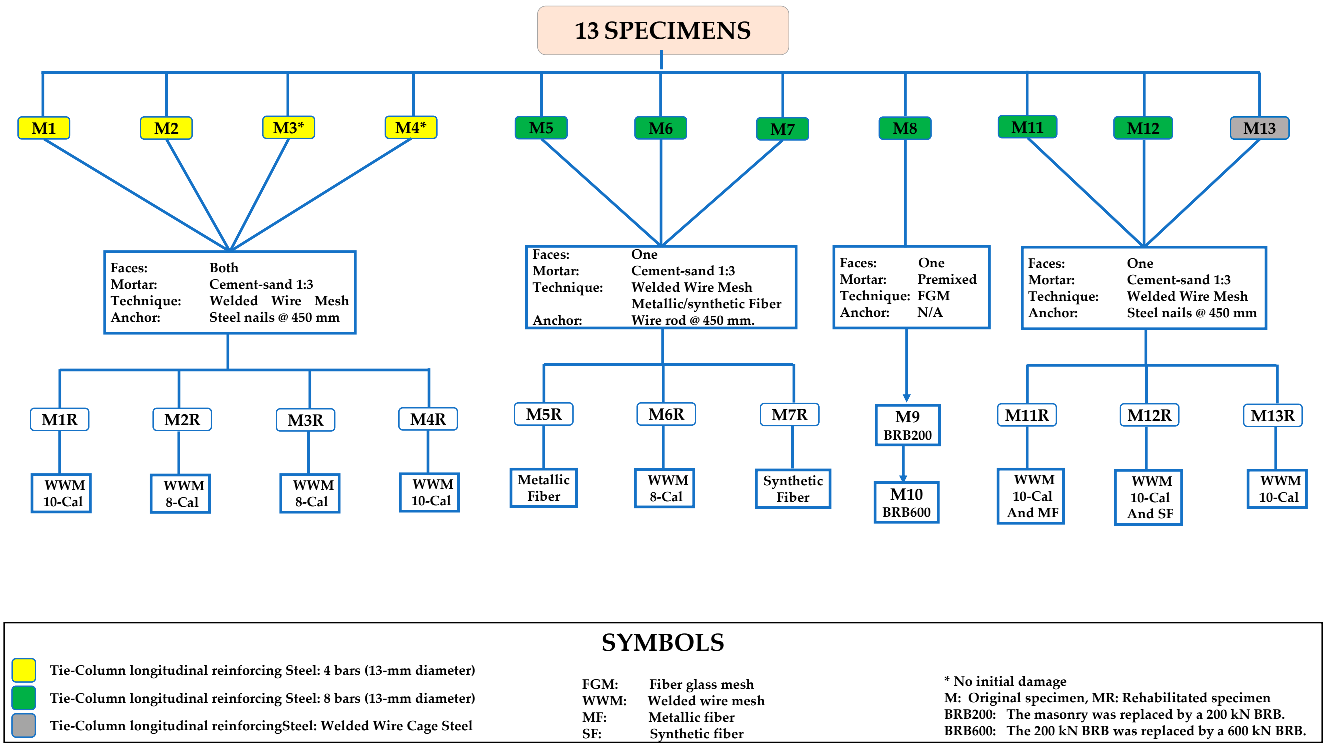

Figure 1. Differences between tested specimens.

2.2. Material Properties

2.2.1. Masonry Units

Masonry units were hand-made solid clay units. Compression tests were conducted on five units sampled randomly from the lot to obtain their mechanical properties according to ASTM C39/C39M-12 [27]. Figure 2 shows some images from the tests. The average value of their compressive strength was 7.84 N/mm^2.

Figure 2. Compression tests of the masonry units.

2.2.2. Mortar

Joint mortar was prepared according to the Mexico City Norms for Design and Construction of Masonry Structures [28], with a cement–sand mixture with a ratio of 1:3 based on volume. To determine the mortar's compressive strength, thirty 50 mm cubes were tested according to the NTCD-Masonry [28]. Photos of cube tests are shown in Figure 3. The average value of the mortar's compressive strength was 13.2 N/mm^2. In addition to the cement and sand mortar for joints, mortar cubes of the mortar used in the rehabilitation were also tested, resulting in the following compressive strengths: 28.6 MPa for Sika Monotop-722 Mur [23], 16.1 MPa for StoneCrete [26], and 23.9 MPa for the cement and sand mortar used to cover the WWMs. In addition to the compressive strength, the modulus of elasticity used was determined following the procedure described by ASTM C469/C469M-10 [29] The experimental values were 1324 MPa for the hand-mixed mortar, 4073 MPa for the StoneCrete mortar, and 8030 MPa for the Sika mortar.

Figure 3. Compression tests of the mortar.

2.2.3. Prism Tests

Masonry compressive strength was determined through testing 18 prisms with dimensions 315 $\times$ 120 $\times$ 240 mm. The prisms were built with five units joined with the same mortar used for the walls, as shown in Figure 4. The tests were conducted in conformance with the Mexican standard NMX-C-464-ONNCCE [30], similar to ASTM E519-15 [31]. The average value of prism compressive strength was 3.44 MPa.

Figure 4. Compression tests of the masonry prisms.

2.2.4. Diagonal Compression Test

Diagonal compression tests were carried out on 11 reduced-scale brick masonry panels, with dimensions of 365 × 120 × 315 mm, to determine the diagonal compression strength of the masonry, as shown in Figure 5. Panels were subjected to a compression load along one of its diagonals. Tests were conducted following the requirements of the Mexican standard NMX-C-464-ONNCCE [30], which is similar to ASTM E519-15 [31]. The average value of diagonal compression strength was 0.60 MPa.

Figure 5. Diagonal compression test.

Diagonal compressive tests were conducted on 12 panels, rehabilitated with mortar on one face, to evaluate the effect of mortar cover on the diagonal compression strength of the masonry. The panels, rehabilitated with cement and sand mortar, had a diagonal compression strength of 1.03 MPa, while the ones rehabilitated with Sika Monotop-722 Mur [23] had a strength of 1.05 MPa. Note that the diagonal compression strength was, on average, 70 percent greater than the strength obtained without mortar cover (i.e., 1 MPa compared to 0.60 MPa).

2.2.5. Concrete Compressive Strength

To determine the concrete compressive strength of the confining elements, standard 150 mm diameter cylinder specimens were tested according to ASTM C39/C39M-12 [27]. Figure 6 shows some pictures taken during the tests. The average compressive strength was 16.8 MPa. This value is typical of masonry construction.

Figure 6. Compression test of the confining elements concrete.

2.2.6. Reinforcing Steel

For the longitudinal reinforcement of the confining elements, deformed steel bars with a nominal yield strength of 420 MPa were used, while the transverse reinforcement had a nominal yield strength of 230 MPa. Figure 7 shows some pictures taken during the placement of electric strain gauges in the steel bars. For specimen M13, the longitudinal and transverse reinforcement was made of a steel welded wire cage. The wire steel had nominal yielding strength of 500 MPa.

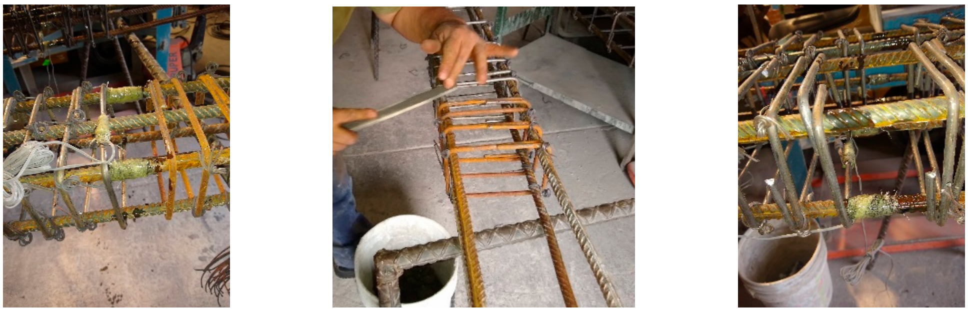

Figure 7. Instrumentation of the reinforcement of the confining elements.

2.2.7. Welded Wire Mesh

WWM used in wall rehabilitation had a nominal yield strength of 500 MPa. Actual properties were measured from three coupons obtained from the wire mesh. Figure 8 shows some pictures taken during the tests. The average yield strength in tension resulted in 494 MPa.

Figure 8. Tensile test of the wire mesh.

2.2.8. Steel and Synthetic Fibers

The steel fibers used for jacketing specimens M5 and M12 were Sika Fiber Xorex [25], which are deformed filaments of steel wire used for reinforcing concrete or mortar. Fiber dimensions were 38 × 2 × 0.5 mm, while their minimum tensile strength reported by the manufacturer was 828 MPa.

Synthetic fibers used in M7 and M11 were Sika Fiber Force PP-48 [24]. They are synthetic polyolefin macro-fibers used for structural concrete or mortar. Fiber dimensions were 48 × 1.37 × 0.34 mm, density of 0.92 g/cm^3, and reported minimum tensile strength of 500 MPa.

Table 2 includes the results obtained in the different material tests. The main dimensions of the tested specimens are also presented, and their average strength.

Table 2. Summary of the results in tests of the different materials.

Material	Size [mm]	Strength [MPa]	Material	Size [mm]	Strength [MPa]
Brick units	60 × 120 × 240	7.8	Concrete for jacketing	150 × 300	40.1
Prisms	120 × 235 × 315	3.44	Concrete for foundation	150 × 300	37.5
Diagonal compression panels	120 × 365 × 315	0.60	Sika Monotop-722 Mur mortar	50 × 50 × 50	28.6
Walls with HM	145 × 365 × 315	1.03	StoneCrete mortar	50 × 50 × 50	16.1
Walls with FGRM	130 × 365 × 315	1.05	Synthetic fiber mortar	50 × 50 × 50	25.0
Walls with SFRM	145 × 365 × 315	1.02	Steel fiber mortar	50 × 50 × 50	22.9
Walls with MFRM	145 × 365 × 315	1.01	Hand-mixed mortar for ME	150 × 300	1205
CS Mortar	50 × 50 × 50	13.24	Synthetic fiber mortar for ME	150 × 300	1355
Wire mesh	L = 600 cm ∅ = 3.43 mm	494	Steel fiber mortar for ME	150 × 300	1413
Concrete for confining elements	100 × 200	16.8	StoneCrete mortar for ME	150 × 300	4073

Symbols: HM = Hand-Mixed mortar; CS = Cement and Sand; FGRM = Fiber Glass-Reinforced Mortar; SFRM = Synthetic Fiber-Reinforced Mortar; MFRM = Steel Fiber-Reinforced Mortar; RC = Reinforced Concrete; ME = Modulus of Elasticity.

2.3. Test Setup

The experimental setup for testing the specimens is schematically shown in Figure 9. Walls were anchored to a reinforced concrete footing, and this, in turn, was fixed to a reaction slab. The load was applied using a hydraulic actuator. The force of the hydraulic actuator was transmitted to the reaction wall using a steel beam fastened to the wall slab. Cao et al. [32] studied the slab influence in dynamic responses through seismic excitations. It was found that structures without slabs had more deformation than those with slabs; that means that the slab has a significant influence on the structure's behavior. Accordingly, the lateral restriction was added to the steel beam to avoid out-of-plane deformation. The beam weighed 15 kN, and a weight of 135 kN was placed on it, which added a total vertical load of 150 kN. The cross-sectional area of the wall was 120 mm × 2500 mm, so the applied vertical stress onto the wall was 0.5 MPa. This axial stress is equivalent to that found in walls in the ground story of a five-story masonry building in Mexico.

2.4. Loading Protocol

The tests were conducted under reversed cyclic loading, following the recommendations by NTC-Masonry [28]. Figure 10 shows the loading protocol, which was applied as follows:

- First, two load cycles (red line) equivalent to 20 percent of the calculated lateral load carrying capacity were applied (i.e., at 26 kN);
- Then, two other load cycles (blue line), equivalent to 40 percent of the wall's calculated strength, were applied (i.e., at 52 kN);
- Finally, incremental displacement-controlled cycles (gray line) were applied to failure;
- At each loading or displacement stage, two load cycles were applied.

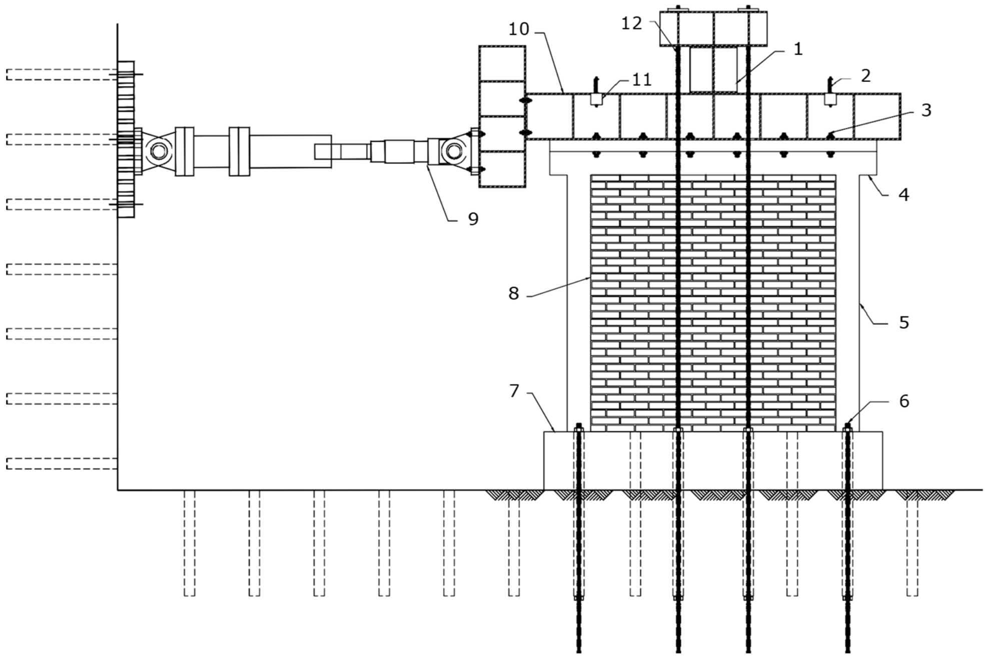

1. Vertical load distribution beam.
2. Out-of-plane bracing.
3. Screw.
4. Tie-beam.
5. Tie-column.
6. Anchor.
7. Concrete beam anchored to the foundation slab.
8. Masonry wall.
9. Hydraulic jack.
10. Horizontal load distribution beam.
11. Wood pole.
12. Tensor

Figure 9. Scheme of the test setup.

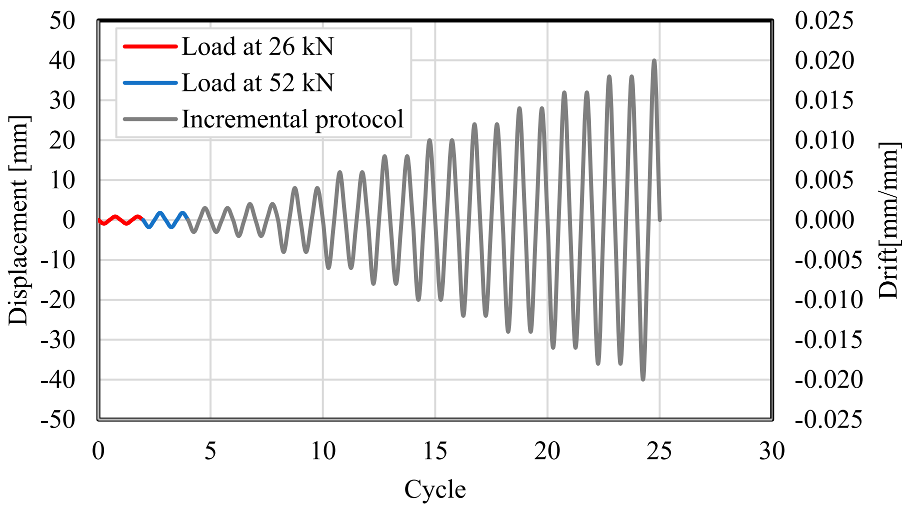

Figure 10. Loading protocol according to NTC-Masonry [28].

Lateral drift, δ, is defined as the applied lateral deformation divided by the height of the wall. In the original walls (without rehabilitation), lateral drifts to δ = 0.0015, 0.002, 0.004, and 0.005 were applied. In the case of the rehabilitated walls, values of lateral drifts to δ = 0.0015, 0.002, 0.004, 0.006, 0.008, 0.010, and so on, with increments of 0.002, were applied until the specimen failure was observed. It is worth mentioning that, initially, an attempt was made to bring the original wall M1 (i.e., without rehabilitation) to drift to δ = 0.006. However, before reaching that drift, a sudden failure occurred at the base of the right tie-column, on the opposite side of the actuator, which generated a lateral drift to δ = 0.008. Due to this incident, the maximum lateral drift was limited to 0.005 for the original walls in the following specimens. The damaged concrete at the base of the tie of specimen M-1 was repaired by concrete replacement.

2.5. Instrumentation

2.5.1. External Instrumentation

The specimens were internally and externally instrumented. The distribution and symbology of the instruments are shown in Figures 11 and 12, respectively. External instruments consisted of load cells and Tokyo Sokki displacement transducers, CDP, with strokes of 100 mm, 50 mm, or 10 mm, with a precision of 0.01 mm. In Figure 11, the load cell to measure the vertical force is identified as FV, while the load cell to measure the horizontal load is FH; the horizontal transducers are marked as H1 to H8, while the vertical instruments are V1 and V2. Transducers D1 and D2 measured the diagonal deformation in the wall. The specimen rotation was measured with the help of R1 and R2. Finally, out-of-plane deformations were monitored with the FP1 and FP2. It is worth mentioning that H1 and H2 served as references for controlling the lateral displacements during the tests.

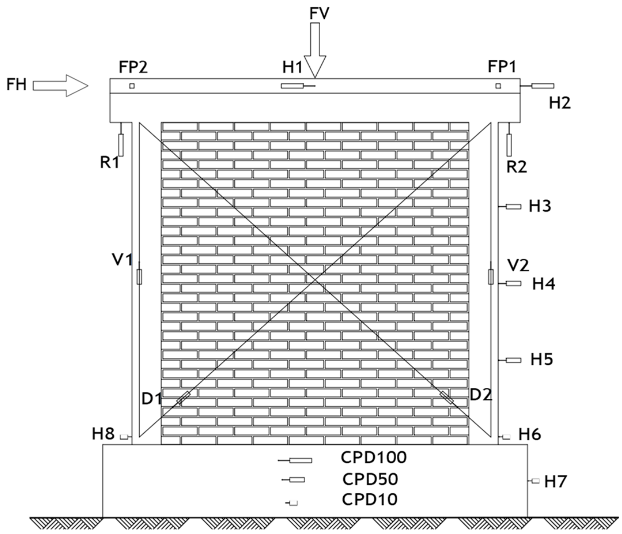

Figure 11. External instrumentation.

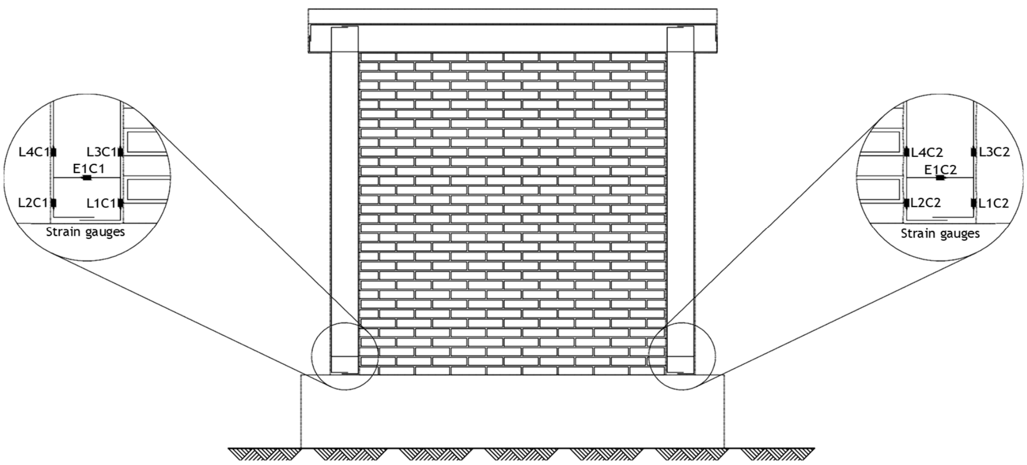

Figure 12. Internal instrumentation with strain gauges.

2.5.2. Internal Instrumentation

Internal instruments (i.e., foil strain gages) were placed in strategic points to measure the stress distribution in the steel reinforcement of the vertical confining elements (C1 and

C2). Strain gauges (L1, L2, L3, L4, and E1) were attached to the reinforcing bars (Figure 12). Some were also placed in the wire mesh of some rehabilitated walls.

3. Construction and Rehabilitation of the Test Specimens

Walls were rehabilitated using mortar cover reinforced with steel WWM, steel fibers, synthetic fibers, fiberglass mesh, and buckling-restrained braces. The main objective of these rehabilitation techniques was to reach or exceed the walls' original strength and deformation capacity. This section first describes the fabrication process of the walls and then their rehabilitation with the techniques described in Section 2.1. Table 1 shows that specimens M3 and M4 were rehabilitated without being initially damaged; M11 and M12 were covered with premixed mortar StoneCrete [26] before being damaged to assess their strength increase due to initial mortar cover. According to Section 2.2.2, the mortar had a compressive strength of 16.13 MPa.

3.1. Construction of Test Specimens

The construction process of specimens is shown in Figure 13. First, the reinforcement of the vertical confining elements was anchored to a precast foundation footing (Figure 13a). Then, the brick units were joined with mortar (Figure 13b) before casting the confining elements against it (Figure 13c). Subsequently, the slab and the horizontal confining element were cast monolithically.

(**a**) (**b**) (**c**) (**d**)

Figure 13. Photographs of the specimens in construction. (**a**) Reinforcement of the vertical confining elements; (**b**) location of brick units; (**c**) wall before casting the confining elements; and (**d**) wall during casting the confining elements.

3.2. Rehabilitation with Mortar Reinforced with Welded Wire Mesh

Specimens M1 to M4, M6, and M11 to M13 were rehabilitated with WWM and mortar. After roughening the masonry surface to a 6 mm amplitude, the WWM was anchored to the wall using either wires or steel nails spaced at 450 mm, as indicated in Table 1. Figure 14a shows a photograph of the anchorage. The mesh was wrapped over the other face to cover 450 mm for efficient anchoring (Figure 14b). Once the rehabilitation was finished (as seen in the rehabilitated specimen of Figure 14c), rehabilitated specimens were tested after 28 days.

(**a**) (**b**) (**c**)

Figure 14. Rehabilitation with welded wire mesh and anchored with wires or steel nails. (**a**) Ancorge of WWM; (**b**) wrapping of the WWM; and (**c**) rehabilitated specimen ready for testing.

3.3. Rehabilitation with Mortar Reinforced with Fibers

Similar to the rehabilitation with welded wire mesh, the specimens' surface was roughened to a 6 mm amplitude to achieve a better bond of the mortar. Steel Sika fiber Xorex (Figure 15a) or Synthetic Sika fiber Force 48 PP DE (Figure 14b) were added to the mortar. Specimens M5 and M12 were rehabilitated with mortar reinforced with steel fibers (with a dosage of 20 kg/m^3), while synthetic fibers were used in specimens M7 and M11 (with a dosage of 10 kg/m^3). Note that specimens M11 and M12 were also rehabilitated with WWM, as indicated in Table 1. Figure 14c shows a picture of the fiber-reinforced mortar during mixing in the lab. Figure 14d shows the application of the mortar on the wall. It is significant to mention that confinement was placed with a U-shaped WWM that surrounded the vertical tie-columns, only 450 mm at each wall edge of the specimens M5 and M7.

(**a**) Metal Fiber (**b**) Synthetic Fiber (**c**) Mortar mix (**d**) Mesh placement

Figure 15. Rehabilitation with synthetic and metal fibers.

3.4. Rehabilitation with Fiberglass Mesh and Premixed Mortar

Figure 16 The rehabilitation process of specimen M8 with fiberglass mesh mortar MonoTop-722 Mur [23] is shown in Figure 16. Figure 16a shows the masonry surface preparation to improve the bond of the mortar. A 5 mm layer of the mortar was placed, on which the mesh was applied; another 5 mm layer of mortar was placed (Figure 16b). Upon completion, a fiberglass anchor was added to each corner of the wall (Figure 16c).

(**a**) Roughening (**b**) Cover (**c**) Fiberglass anchor (**d**) Reduced-scale wall

Figure 16. Rehabilitation of M8 with fiberglass mesh reinforced mortar.

Three masonry panels were built, as described in Section 2.2.4, to estimate the mesh's contribution to the rehabilitated wall's lateral strength. One face of the panels was covered with the same rehabilitation process as specimen M8 (Figure 16d).

3.5. Rehabilitation with Buckling-Restrained Braces (BRB)

As a part of this research project, specimens M9 and M10 were rehabilitated with buckling-restrained braces (BRB) to assess the possible advantages or disadvantages of this system. The masonry panel of specimen M8 was removed, leaving a simple frame made of the small confining elements (Figure 17a). For the new specimen, now called M9, the upper-left and lower-right joints were jacketed with steel plates (as seen in Figure 16b), and a BRB with a yield axial strength of 200 kN was connected (Figure 16c). Once the tests of specimen M9 were completed, the connection plates and the BRB were removed, with the intention of reusing the frame. This new frame was now called specimen M10. For this, vertical and horizontal elements were rehabilitated by reinforced concrete jacketing. The new dimensions were 350 × 350 mm for the vertical elements and 350 × 300 mm for the horizontal element.

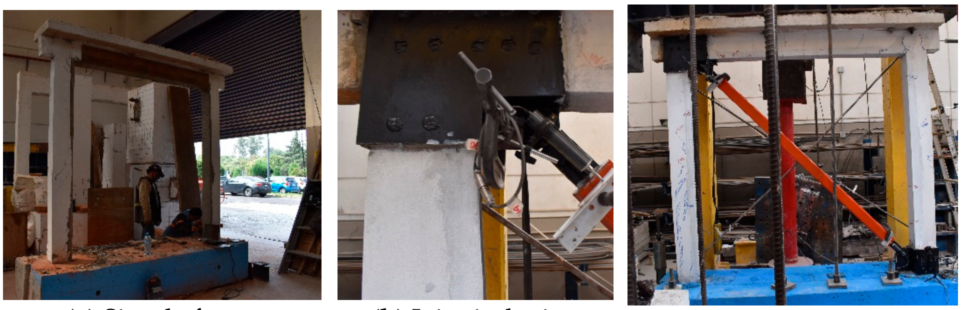

(**a**) Simple frame (**b**) Joint jacketing (**c**) Frame with BRB

Figure 17. Rehabilitation of M9 with a buckling-restrained brace (BRB).

Figure 18 shows the rehabilitation process of specimen M10. The concrete of the existing elements was roughened to 6 mm amplitude (Figure 17a) to improve the bond between the existing and new concrete. Subsequently, steel reinforcement (Figure 17b) was placed, and concrete was cast (Figure 17c). Note that the columns were cast first, then the beam (Figure 17d). The BRB was connected using a steel frame, joined to the RC jacket with steel connectors designed to work in shear. The BRB had a yield axial strength of 600 kN.

(**a**) (**b**) (**c**) (**d**)

Figure 18. Rehabilitation of M10 with restrained buckling braces. (**a**) Concrete roughening; (**b**) placing of steel reinforcement; (**c**) casting of concrete for columns; and (**d**) preparation of the beam after casting the columns.

4. Experimental Results

In this section, the results obtained from the experimental tests are presented. The letter "R" is used to refer to a rehabilitated specimen. For example, M1R refers to specimen M1 rehabilitated.

4.1. Assessment of Cracking

During the tests, cracks were marked with different colors. Red was used when the hydraulic actuator was under compressive loads (push cycles), and blue was used under tension loads (pull cycles). Figure 19 presents pictures of the crack patterns and the maximum crack width noted as W_c, measured in the damaged specimens at the end of the tests. In general, a uniform distribution of cracks is observed in the specimens rehabilitated with WWM. This observation shows the efficiency of this rehabilitation technique in distributing damage in the wall and avoiding the concentration of damage along a single crack.

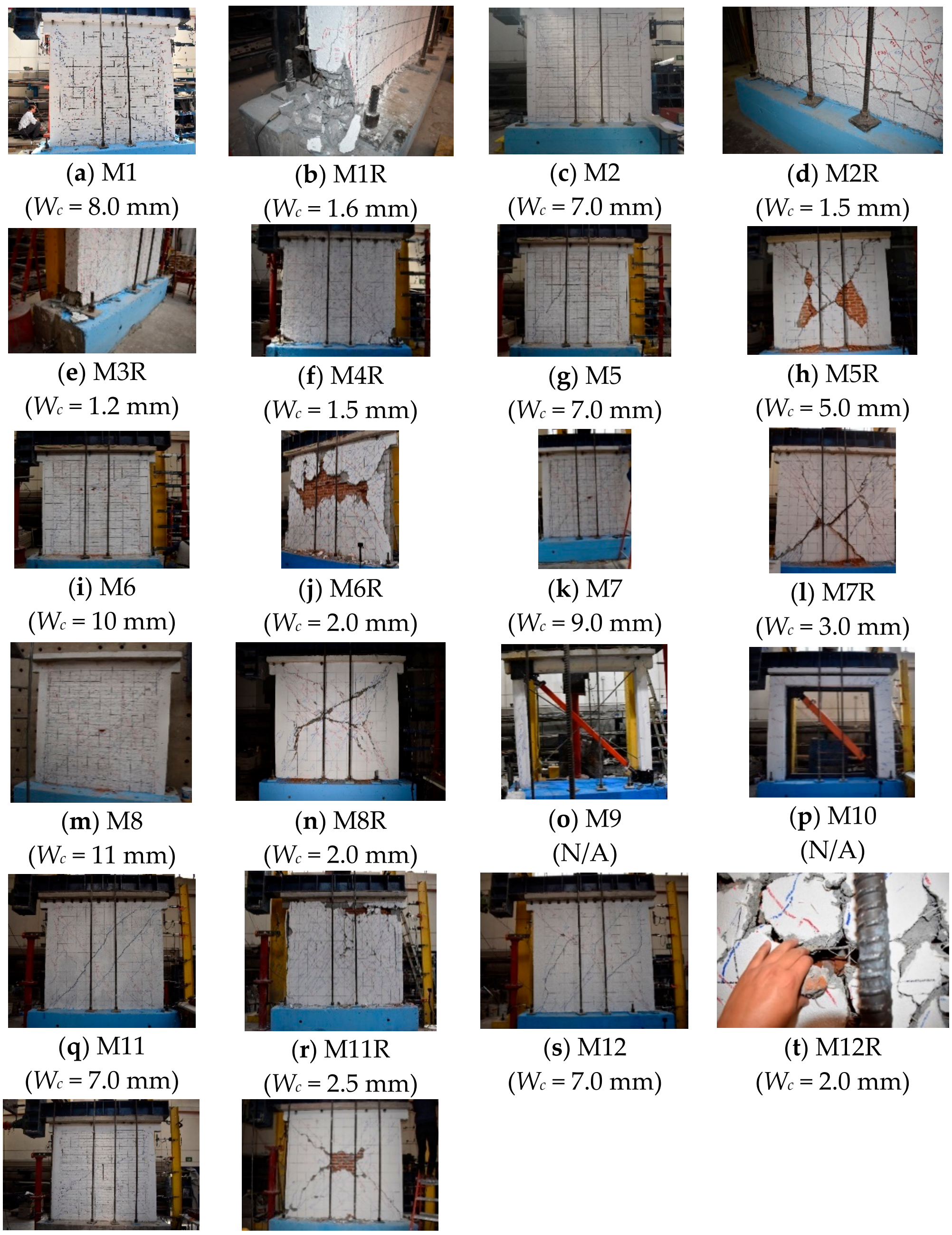

(**a**) M1 (W_c = 8.0 mm)
(**b**) M1R (W_c = 1.6 mm)
(**c**) M2 (W_c = 7.0 mm)
(**d**) M2R (W_c = 1.5 mm)
(**e**) M3R (W_c = 1.2 mm)
(**f**) M4R (W_c = 1.5 mm)
(**g**) M5 (W_c = 7.0 mm)
(**h**) M5R (W_c = 5.0 mm)
(**i**) M6 (W_c = 10 mm)
(**j**) M6R (W_c = 2.0 mm)
(**k**) M7 (W_c = 9.0 mm)
(**l**) M7R (W_c = 3.0 mm)
(**m**) M8 (W_c = 11 mm)
(**n**) M8R (W_c = 2.0 mm)
(**o**) M9 (N/A)
(**p**) M10 (N/A)
(**q**) M11 (W_c = 7.0 mm)
(**r**) M11R (W_c = 2.5 mm)
(**s**) M12 (W_c = 7.0 mm)
(**t**) M12R (W_c = 2.0 mm)
(**u**) M13 (W_c = 5.0 mm)
(**v**) M13R (W_c = 5.0 mm)

Figure 19. Pictures of the crack distribution on the specimens.

Figure 19b,e,f shows significant damage at the vertical elements' bottom edges. This effect occurred due to the strengthening of the specimens on both sides, which caused a change in the failure mechanism. Instead of a diagonal tension failure of masonry, failure was controlled by shear friction, causing damage to the wall toe due to flexo-compression on the vertical confining elements.

A quantitative evaluation of the cracks is presented later in Section 4.6, where each specimen's peak and residual crack are evaluated and compared with the lateral deformation.

4.2. Load-Deformation Curves

The hysteresis loops of the original and rehabilitated specimens are presented in Figure 20. The vertical axis shows, in kN, the lateral load applied to the walls, while the horizontal axis shows its lateral drift (i.e., the lateral displacement divided by the wall's height) in mm/mm. The hysteresis loops are shown in a gray line. The dashed black lines indicate the envelope of the first loading cycle, while the solid black lines show the envelope of the second loading cycle. The red, horizontal dashed lines show the nominal calculated strength according to NTC-Masonry [28]. Calculated strengths used measured material properties and assumed a strength reduction factor equal to 1.0. It can be seen that, except for specimen M13, which was built with a steel welded wire cage, all the specimens reached greater strengths than the calculated values by NTC-Masonry [28]. In addition, it is seen that the load and deformation capacity of the rehabilitated specimens was significantly higher than that of the original specimens. It is observed that the pinching behavior, associated with a reduced dissipated hysteretic energy under cyclic loading, appears in the hysteresis curves of all specimens except M9 and M10. It is significant to mention that pinching is a characteristic of several structural systems [33], including confined masonry walls, because of material degradation under shear when subjected to cyclic loads. The effect of the second loading cycle on strength and stiffness is small.

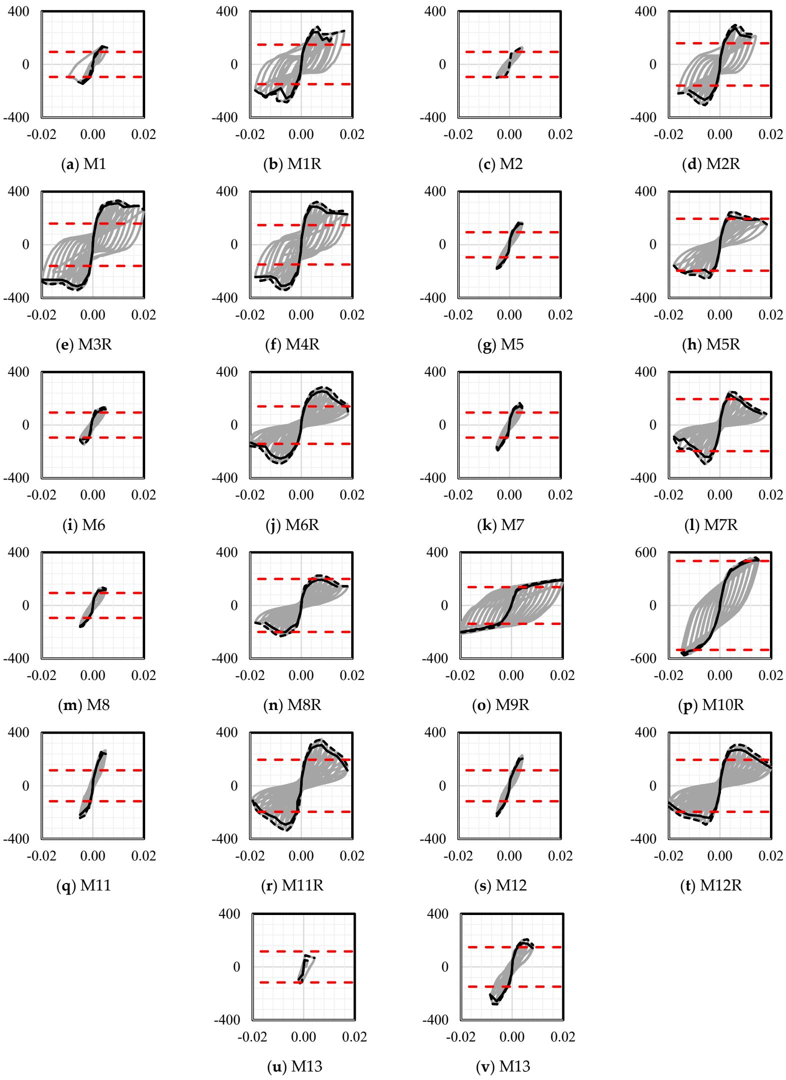

Figure 20. Load-drift curves. Vertical axes in kN and horizontal axes in mm/mm.

4.3. Backbone Curves

Backbone curves were obtained to represent the load-deformation curves of Section 4.2. First, a bilinear model was calculated up to the maximum load supported by the specimen, P_m, based on FEMA 356 [34], which specifies that:

(a) The area under the curve of the equivalent bilinear model that of the load-deformation envelope obtained experimentally must be equal;

(b) The ascending branch of the equivalent bilinear model must intersect the experimental envelope at 0.6 P_y, where P_y is the bilinear model yield load point.

As seen in Figure 20, the rest of the points of the multilinear curve are (0.8 P_m, $\delta_{0.8}$) and (P_u, δ_u), where 0.8 P_m corresponds to the load point at which the strength has been reduced by 20 percent of the maximum load; $\delta_{0.8}$ is the lateral deformation associated with 0.8 P_m; δ_y and δ_m are the lateral deformations associated, respectively, to P_y and P_m; and P_u and δ_u are the last load and deformation that the specimen endured before failure. In Figure 21, the stiffness of each branch is also represented, while the values obtained for each specimen are shown in Table 3. The stiffness ratios α_1 and α_2 are also shown in the table.

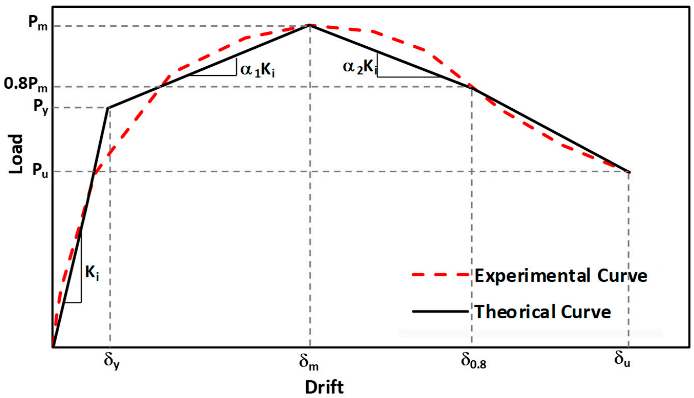

Figure 21. Backbone curve and its structural characteristics.

Table 3. Summary of the structural properties of the specimens.

ID	Dir	P_y [kN]	P_m [kN]	$P_{0.8}$ [kN]	P_u [kN]	δ_y *Bilinear*	δ_m *Trilinear*	$\delta_{0.8}$ *Trilinear*	δ_u *Trilinear*	K_i [kN/mm]	α_1	α_2
M1	(+)	118.2	138.0	126.0	110.4	0.0012	0.0036	0.0056	0.0082	40.9	0.19	0.07
	(−)	132.4	147.0	132.0	117.6	0.0012	0.0039	0.0057	0.0074	42.7	0.02	0.01
M1R	(+)	240.6	283.5	226.8	226.8	0.0022	0.0064	0.0085	0.0168	43.1	0.16	0.22
	(−)	243.3	284.7	227.8	227.8	0.0021	0.0056	0.0099	0.0181	46.7	0.16	0.07
M2	(+)	105.2	130.0	130.0	130.0	0.0008	0.0048	0.0048	0.0048	51.8	0.10	0.03
	(−)	92.5	100.0	101.0	101.0	0.0010	0.0020	0.0050	0.0050	36.6	0.36	0.03
M2R	(+)	253.5	297.0	237.6	237.6	0.0022	0.0059	0.0098	0.0140	45.5	0.17	0.13
	(−)	255.8	306.5	245.2	245.2	0.0021	0.0058	0.0111	0.0163	48.0	0.19	0.09
M3R	(+)	303.7	333.0	266.4	266.4	0.0023	0.0100	0.0197	0.0200	52.5	0.05	0.05
	(−)	306.4	340.0	272.0	272.0	0.0020	0.0061	0.0200	0.0200	60.2	0.10	0.03
M4R	(+)	291.4	323.0	258.4	258.4	0.0017	0.0056	0.0056	0.0056	68.9	0.00	0.00
	(−)	310.6	340.0	272.0	272.0	0.0021	0.0061	0.0114	0.0163	60.5	0.09	0.08
M5	(+)	148.6	169.5	168.0	168.0	0.0015	0.0036	0.0045	0.0045	38.6	0.17	0.01
	(−)	163.6	180.5	180.5	180.5	0.0022	0.0050	0.0050	0.0050	29.1	0.18	0.03
M5R	(+)	210.4	249.0	199.2	199.2	0.0021	0.0055	0.0131	0.0183	39.9	0.11	0.07
	(−)	221.1	254.0	203.2	203.2	0.0020	0.0060	0.0154	0.0180	44.3	0.10	0.05
M6	(+)	122.8	133.0	133.0	133.0	0.0012	0.0050	0.0050	0.0050	41.2	0.05	0.01
	(−)	128.8	147.0	117.6	117.6	0.0021	0.0036	0.0049	0.0050	24.4	0.37	0.38

Table 3. *Cont.*

ID	Dir	P_y [kN]	P_m [kN]	$P_{0.8}$ [kN]	P_u [kN]	δ_y *Bilinear*	δ_m *Trilinear*	$\delta_{0.8}$ *Trilinear*	δ_u *Trilinear*	K_i [kN/mm]	α_1	α_2
M6R	(+) (−)	236.1 229.4	284.5 292.0	227.6 233.6	227.6 233.6	0.0020 0.0024	0.0080 0.0081	0.0132 0.0134	0.0181 0.0200	47.1 39.0	0.10 0.16	0.09 0.11
M7	(+) (−)	148.2 150.6	166.0 190.0	132.8 152.0	132.8 152.0	0.0016 0.0014	0.0040 0.0046	0.0049 0.0050	0.0049 0.0050	37.2 43.6	0.15 0.20	0.02 0.49
M7R	(+) (−)	173.9 211.2	251.5 295.0	201.2 236.0	201.2 236.0	0.0014 0.0020	0.0037 0.0059	0.0086 0.0086	0.0181 0.0180	48.2 42.6	0.28 0.20	0.06 0.21
M8	(+) (−)	124.7 150.2	134.5 161.0	126.0 161.0	126.0 161.0	0.0017 0.0023	0.0037 0.0050	0.0050 0.0050	0.0050 0.0050	28.7 25.7	0.16 0.09	0.02 0.02
M8R	(+) (−)	188.5 189.1	225.0 231.0	180.0 184.8	180.0 184.8	0.0017 0.0018	0.0062 0.0080	0.0130 0.0124	0.0181 0.0180	44.3 41.7	0.12 0.07	0.06 0.10
M9	(+) (−)	170.3 182.2	195.0 202.6	193.0 202.6	193.0 202.6	0.0027 0.0053	0.0200 0.0199	0.0201 0.0199	0.0201 0.0199	25.0 18.6	0.04 0.10	0.10 0.19
M10	(+) (−)	486.6 505.3	541.0 563.5	518.0 536.5	518.0 536.5	0.0037 0.0033	0.0141 0.0140	0.0150 0.0150	0.0150 0.0150	52.0 61.7	0.08 0.14	0.04 0.05
M11	(+) (−)	265.5 217.3	267.0 242.0	267.0 242.0	267.0 242.0	0.0029 0.0019	0.0050 0.0050	0.0050 0.0050	0.0050 0.0050	36.7 46.9	0.02 0.13	0.11 0.06
M11R	(+) (−)	279.6 263.2	349.5 340.0	279.6 272.0	279.6 272.0	0.0016 0.0016	0.0060 0.0058	0.0120 0.0115	0.0180 0.0190	68.1 66.4	0.15 0.16	0.06 0.07
M12	(+) (−)	218.5 194.1	230.0 228.5	230.0 228.5	230.0 228.5	0.0033 0.0025	0.0050 0.0050	0.0050 0.0050	0.0050 0.0050	26.7 31.6	0.20 0.26	0.04 0.05
M12R	(+) (−)	253.5 239.2	310.0 293.0	248.0 234.4	248.0 234.4	0.0019 0.0020	0.0061 0.0055	0.0134 0.0152	0.0200 0.0200	53.3 48.2	0.14 0.18	0.06 0.05
M13	(+) (−)	77.4 119.5	87.0 122.5	68.0 122.5	68.0 122.5	0.0005 0.0007	0.0007 0.0015	0.0042 0.0015	0.0042 0.0015	66.1 65.0	0.58 0.04	0.00 0.01
M13R	(+) (−)	190.0 240.8	208.0 281.0	165.0 208.5	165.0 208.5	0.0019 0.0021	0.0060 0.0058	0.0081 0.0086	0.0081 0.0086	39.7 45.3	0.08 0.18	0.01 0.15

4.4. Stiffness Degradation

A highly relevant parameter for masonry structures is the lateral stiffness, K_{eff}, and degradation. In this research project, the peak-to-peak stiffness of each cycle was calculated, as shown schematically in Figure 22.

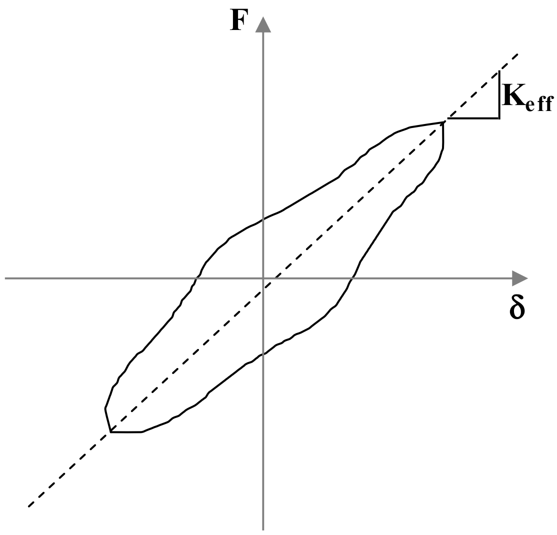

Figure 22. Peak-to-peak stiffness.

Figure 23 plots the values of the peak-to-peak stiffness, measured experimentally. The vertical axis represents the stiffness value in kN/mm, while the horizontal axis shows the lateral drift in mm/mm. Please note that the dashed lines in blue represent the stiffness of the rehabilitated specimens, while the solid lines correspond to the original specimens, that is, before rehabilitation. The horizontal black line represents the calculated stiffness value, previously calculated following the recommendations by the NTC-Masonry [28].

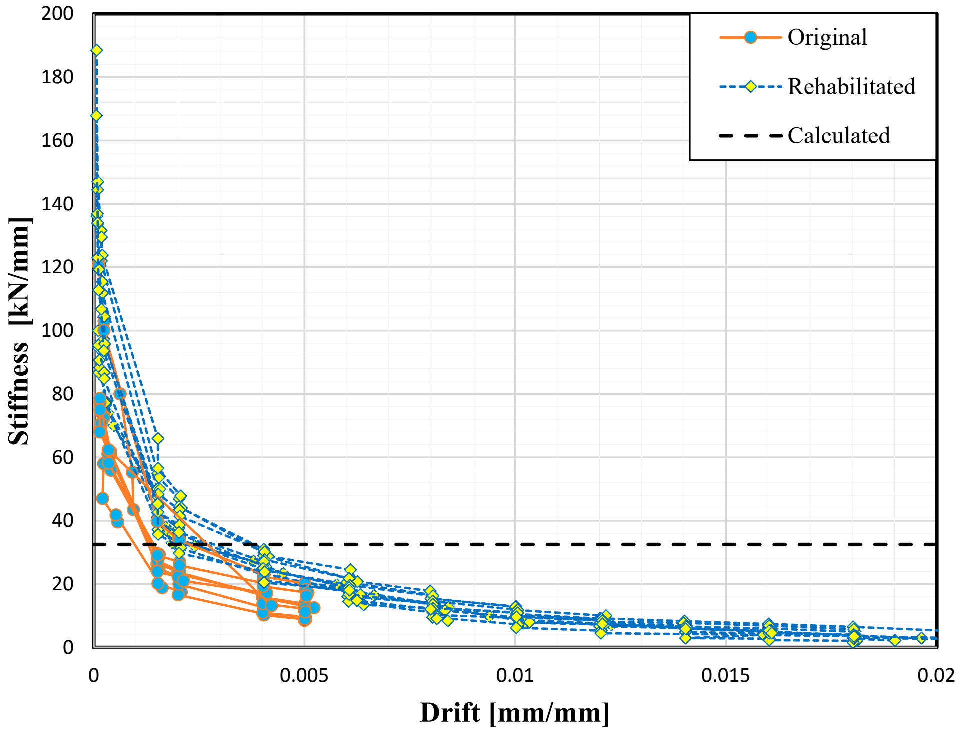

Figure 23. Stiffness and lateral drift per cycle.

It is observed that the initial stiffness observed experimentally is significantly higher than the calculated values. However, as the deformation demand increases, lateral stiffness drops drastically to become smaller than the calculated value at large deformations. For example, most specimens have a smaller stiffness than the calculated value at drifts larger than 0.0025. At a 0.005 drift, all the specimens have stiffnesses smaller than the calculated based on elastic theory. The rehabilitated walls tend to have a greater stiffness than the original specimens, which is due, among other factors, to the contribution of the mortar with which they were rehabilitated. As observed in previous tests, stiffness decay follows a parabolic trend.

4.5. Energy Dissipation

Depending on the material they are made of structures can dissipate energy through different mechanisms. For masonry structures, the following mechanisms can be considered: cracking, the friction generated along the cracks, relative sliding of masonry units, and steel reinforcement yield if applied. The experimental results allow for calculating the energy dissipation capacity for each specimen. That energy corresponds to the area within a hysteresis loop. Figure 24 schematically represents the energy dissipated in a load-deformation cycle (as depicted from the shaded area).

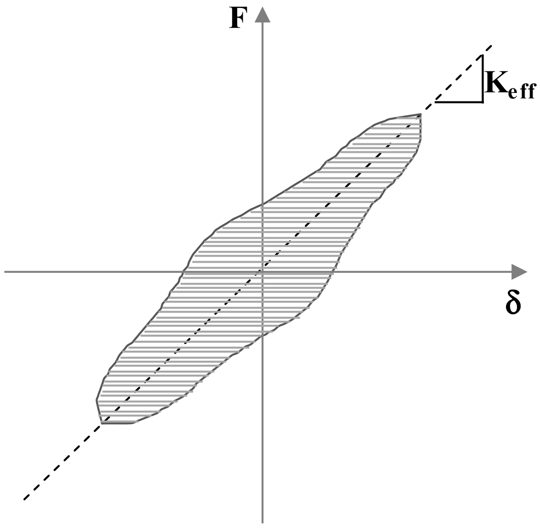

Figure 24. Schematic representation of the dissipated energy calculation.

Figure 25 shows the cumulative energy dissipated by the specimens. It is noted that the rehabilitated walls dissipated energy (in a dashed line) is significantly larger than that of the original specimens (in a continuous line). Specimens M9 and M10 had the highest cumulative energy, i.e., 264 kN-m and 213 kN-m, respectively.

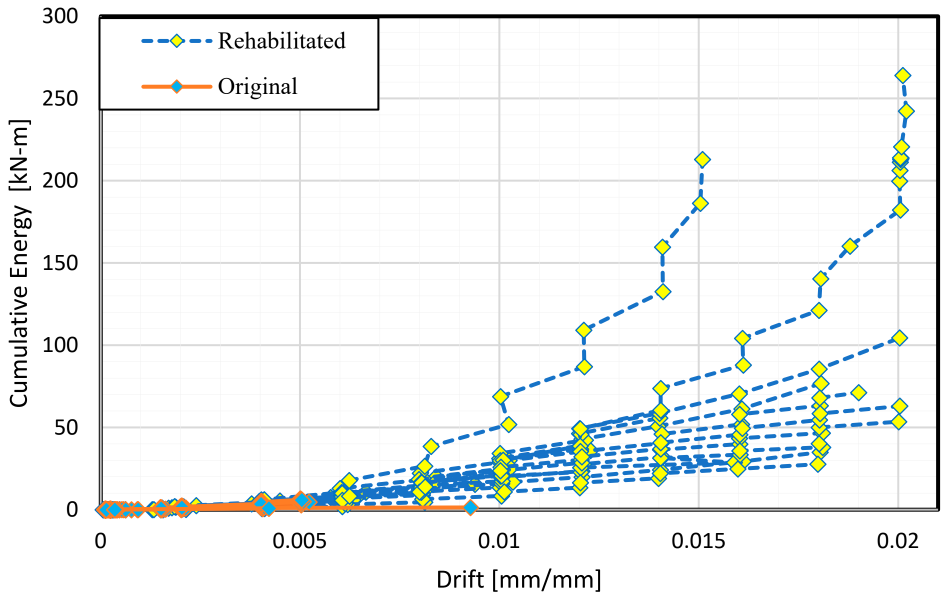

Figure 25. The energy dissipated by the tested specimens.

4.6. Crack Widths

Widths of peak and residual cracks were measured during the tests (Figure 26). Solid circles indicate peak crack widths and empty circles show residual crack widths. In the figure, the vertical axis is the maximum crack width in mm, while the horizontal axis is the lateral drift applied to the specimen during the tests. Linear trend lines were added for illustration purposes. Three observations are precise: (1) crack widths grow with drift; (2) rehabilitated specimens had a smaller peak and residual crack widths than the original specimens; and (3) generally, the residual crack widths are about half of the peak crack widths.

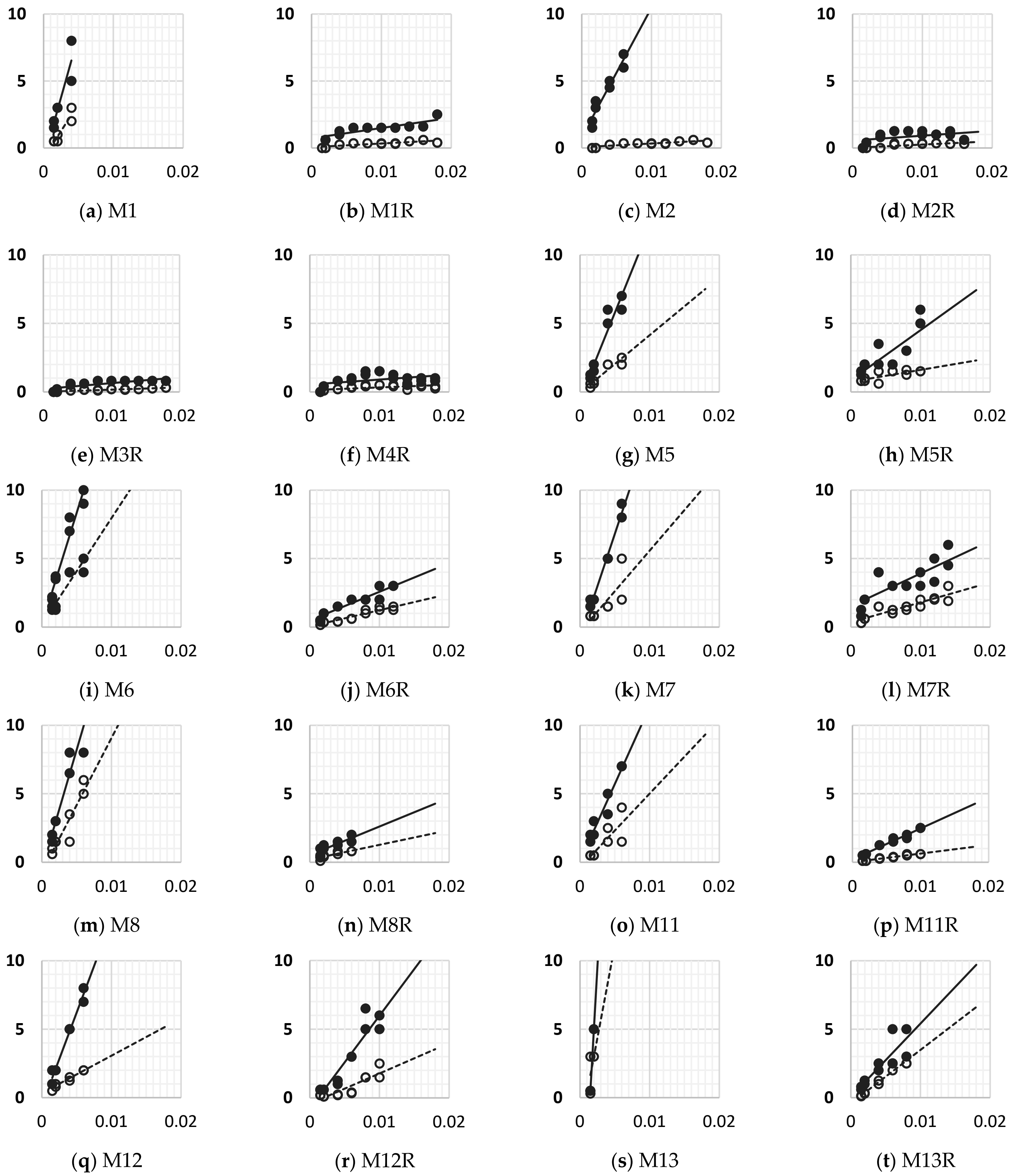

Figure 26. Crack widths. Residual cracks in empty circles and peak cracks in solid circles.

5. Discussion

5.1. General Aspects

The strength of each specimen is plotted in Figure 27. Black columns represent the strength of specimens tested in their original state, while the strength of the rehabilitated specimens is shown through white columns. It is observed that the original specimens had lower strengths, with values around 150 kN, while the rehabilitated specimens reached significantly larger strengths. The M10R specimen, rehabilitated with a BRB of 600 kN at yielding, was the one that presented the highest strength. Note that the measured lateral strength was smaller than 600 kN due to the inclination angle, which was 45°. Specimens M3R, M4R, and M11R were the subsequent specimens that achieved the highest strength, with values close to 350 kN. Then, the specimens M1R, M2R, M6R, M7R, M12R, and M13R had a strength close to 300 kN, followed by the specimens M5R, M8R, and M9R that presented strengths greater than 200 kN. M3R and M4R specimens were strengthened undamaged, while all others were damaged before rehabilitation. Specimens M1R to M4R were rehabilitated with WWM and mortar on both faces, while M5R to M13R were rehabilitated on one face only. Additionally, note that the original specimens M11 and M12 had an average strength of 240 kN, higher than the rest of the original walls because they were covered with simple mortar before being tested in their original state. Therefore, the increase in their strength was due to the contribution of the mortar cover.

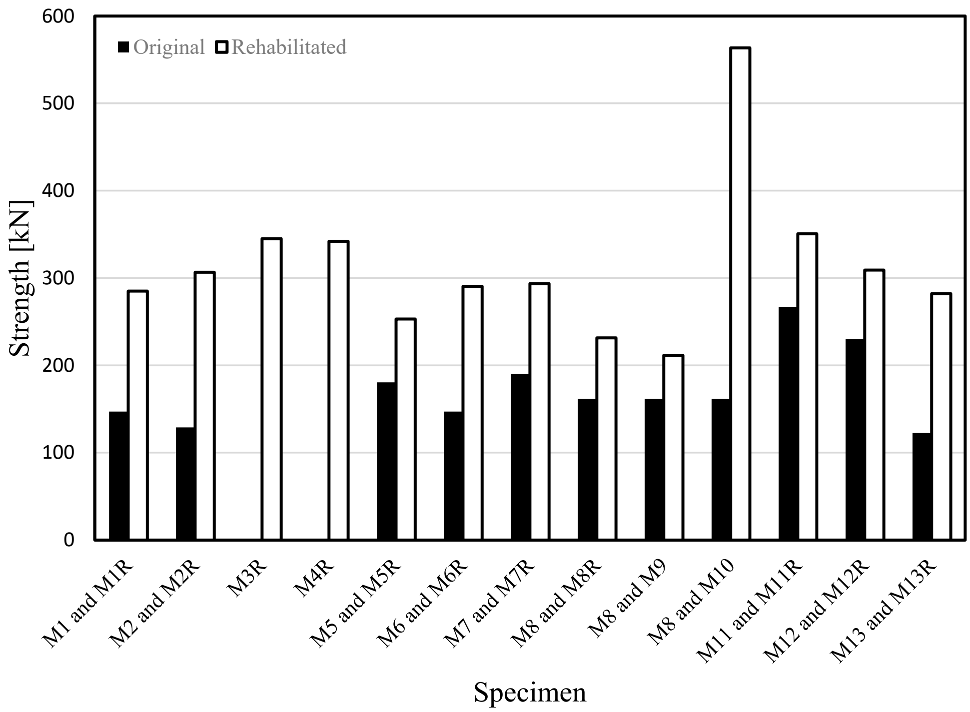

Figure 27. Rehabilitation effects on the strength.

The lateral deformation developed by each specimen is shown in Figure 28. For the rehabilitated specimens, these lateral deformations correspond to a loss of strength by 20 percent. This value was considered according to FEMA P-795 [35], which establishes that this reduction could reasonably correspond to the imminent failure of a wall. It is clarified that the lateral deformation of the original specimens (i.e., not strengthened) is represented by black columns. Note that the original specimens, except M1 and M13, were tested to a drift of 0.005. Specimen M1 was the first to be tested and served as a reference to control the level of initial damage; therefore, its drift in Figure 27 corresponds to a loss of strength by 20 percent of the peak strength.

Similarly, the drift of specimen M13 corresponds to a loss of strength of 20 percent because it failed prematurely. The results show that the rehabilitated specimens had a large deformation capacity, with values greater than 0.01 in most cases and almost reaching 0.02 in some cases. Exceptions are specimens M7R and M13R, which had values smaller than 0.01 because M7R had a rapid degradation of strength, and M13R had a small amount of confinement in its vertical elements because they were reinforced with welded-wire cages.

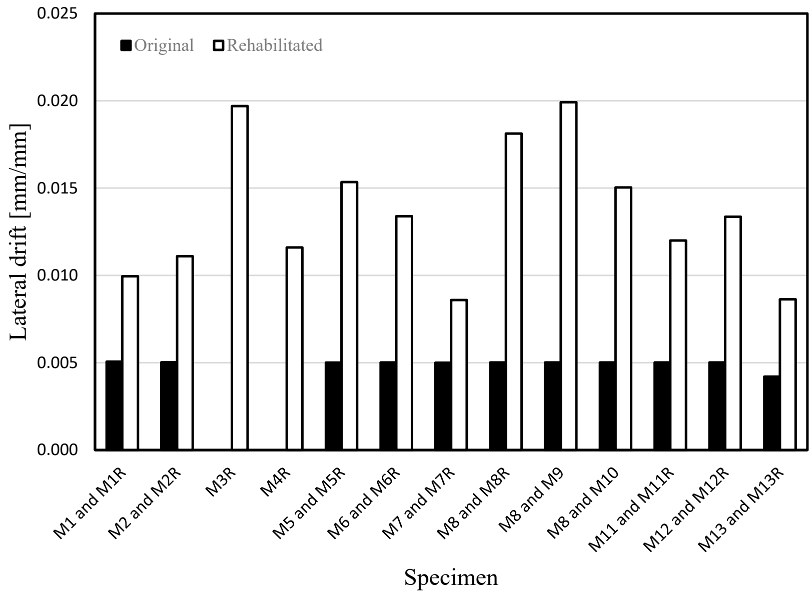

Figure 28. Effect of rehabilitation on lateral deformation capacity (Lateral deformation at 0.8 P_m, as defined in Figure 21).

For illustration purposes, the ultimate lateral drift is also plotted in Figure 29. Even though some of the literature (such as FEMA P-795 [35]) recommends stopping the tests when there is a strength loss by 20 percent of the peak value, it was decided to continue the tests to bring the rehabilitated specimens to their ultimate failure, which is the point where the walls lost their vertical loading capacity. The results were interesting since they show that most of the specimens reached levels of drift between 0.015 and 0.020, which is a substantial value considering that they are masonry walls. As a reference, the Mexico City seismic design standard (NTC-Seismic [36]) limits the maximum drifts to 0.010 when there is horizontal steel reinforcement within the bed joints of the confined masonry wall or 0.005 for conventional confined masonry. The only specimen that, even when rehabilitated, did not reach values greater than 0.010 was the M13R, which was built with prefabricated welded-wire steel cages. However, it doubled its original deformation capacity, which is acceptable for rehabilitating deficient structures.

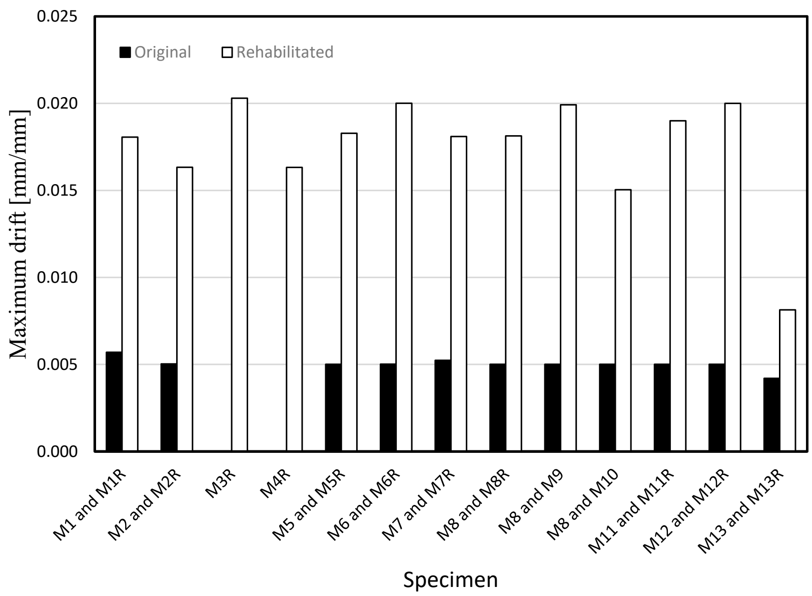

Figure 29. Effect of rehabilitation on lateral deformation capacity (Maximum deformation).

5.2. Effects of the Initial Damage

Specimens M1R and M4R were rehabilitated with mortar, reinforced with 10-cal WWM, designated as $6 \times 6 - 10/10$ (6-in. −150 mm- wire spacing, and 10-cal horizontal and vertical wires). The strength of specimen M4R reached 340 kN, while that of specimen M1R reached 285 kN. That is a difference of 19 percent. Indeed, the initial damage had a significant effect on the lateral strength of the walls. Specimens M2R (initially damaged) and M3R (initially undamaged), rehabilitated using 8-cal welded wire mesh, reached 297 kN and 340 kN. That is a difference of 15 percent.

Regarding lateral deformations, specimens M1R and M4R reached 0.0085 and 0.0116, respectively, while M2R and M3R reached 0.0099 and 0.019, respectively.

5.3. Effects of the Area of Steel of the Wire Mesh

By comparing the strengths of specimens M1R (rehabilitated with 10-cal mesh) and M2R (rehabilitated with 8-cal mesh), M2R resisted 8 percent more than M1R. The steel reinforcement area influences the strength. The greater the amount of steel reinforcement, the more significant the increase in strength. The NTC-Masonry [28] provides an equation to consider the contribution of the area of steel reinforcement to the lateral strength. Indeed, the strength is asymptotic to the sliding capacity of the wall.

5.4. Effects of the Type of Wire Mesh Anchorage

When comparing the results of the M6R specimen, which had a wire anchor, with other specimens with nail anchors (e.g., M11R or M12R), no significant difference related to the type of anchor was observed. Indeed, having roughened the masonry allowed an adequate transfer of shear forces between the wall and the reinforcing mortar, so it could be argued that the anchors had little participation. It is recommended to always remove any plaster and roughen the masonry to 6 mm amplitude and use the anchors that are considered adequate from a constructive point of view.

5.5. Effects of Fibers Combined with Wire Mesh

M11 and M12 walls were initially covered with a 25 mm layer of premixed mortar StoneCrete [36]. Afterward, all the mortar was removed, and the specimens were rehabilitated with 8-cal wire mesh and a mixture of mortar and synthetic fibers for M11R or steel fiber for M12R. Original specimens M11 and M12 reached an average strength of 240 kN, higher than that of other similar walls, because of the contribution of the StoneCrete [26] mortar. Therefore, the relative increase after rehabilitation was less significant than in other cases. However, when combining WWM and fibers, the strength had an average value of 330 kN. In addition, when M11R and M12R are compared against M5R and M7R, which were only rehabilitated with synthetic or steel fibers, respectively. The two latter had an average strength of 273 kN; it is seen that adding the welded wire mesh increased the strength by about 20 percent, which supports the adequacy of combining fibers and WWM.

Regarding lateral deformation capacity, M11R and M12R walls exceeded that of specimens M5R and M7R by 7 percent. Although no conclusive result can be given, a slight trend shows an increase in the deformation capacity due to the combination of fibers (synthetic or metallic) and welded wire mesh.

5.6. Effects of Buckling-Restrained Braces

As discussed in Section 3.5, specimens M9R and M10R were rehabilitated with a BRB. BRB was connected after demolishing the masonry panel from the M8R specimen, leaving only the frame formed by the confinement elements. Additionally, for the M10R specimen, the columns and the beam were rehabilitated with reinforced concrete jacketing because a higher capacity BRB was used.

Regarding lateral load capacity, specimens M9R and M10R had either smaller or greater capacity than other rehabilitated specimens. Furthermore, that is because the BRB of specimen M9R had a reduced yielding strength (200 kN), while that of specimen M10R had a larger one (600 kN). Indeed, the advantage of using BRBs for rehabilitation purposes is that the strength capacity of the BRBs can be tuned (or controlled) to a target value.

Regarding lateral deformation capacity, specimens M9R and M10R were tested at target drifts of 0.020 and 0.015. Specimen M10R was tested at smaller deformations because it had larger concrete elements, which presented significant damage during the tests. The results of these specimens were interesting as they showed BRB had high deformation and energy dissipation capacity. Indeed, and amongst other cases, they may be suitable for rehabilitating structures when weight (or mass) must be removed so that masonry can be removed and replaced by BRBs. According to the hysteresis loops, unlike the other specimens, these two presented wide and stable hysteretic cycles and did not present stiffness or strength degradation. Some stiffness degradation was seen due to the cracking of the concrete elements that formed the frame, especially in specimen M10R, because it had a more robust BRB.

5.7. Effects of Prefabricated Steel Welded Wire Cage

Specimen M13 was built with a prefabricated steel welded wire cage in the vertical confining elements. The reinforcement is commercially known as welded wire reinforcing cages. Wall rehabilitation was conducted with mortar and 10-cal welded wire mesh ($6 \times 6 - 10/10$). It is seen that the original specimen reached a low strength value (122.5 kN) because the provided longitudinal reinforcement quantity was smaller than the minimum required by NTC-Masonry [28]. However, after the rehabilitation, the strength was 282 kN (2.3 times higher than that of the original wall), evidencing the efficiency of the rehabilitation technique. Certainly, deficient walls, built with welded wire reinforcing cages, can efficiently be rehabilitated with welded wire mesh to improve their seismic capacity.

In terms of lateral deformation, the original specimen went from 0.0042 to 0.0081 after the rehabilitation, almost doubling. Certainly, the specimen greatly benefitted from the rehabilitation.

5.8. Comparison of the Rehabilitation Costs

The rehabilitation cost of the studied techniques was estimated and compared. A comparison of the costs at the time when this paper was written is presented in Table 4. More details may be found in Lubin [37]. The most economical technique, in terms of cost per kN of strength and per unit of cumulative energy, was the combination of 8-cal welded wire mesh with steel or synthetic fibers ($373 MXN per m^2), followed by single face jacketing with 8-cal welded wire mesh and mortar or single face with either synthetic or steel fibers and mortar.

Table 4. Comparative table of costs of the rehabilitation techniques studied.

Technique	Cost per m^2 [$ MXP]	Strength [kN]	Cumulative Energy [kN-mm]	Cost per kN [$ MXP]	Cost per kN-mm
Both faces, 10-cal wire mesh with mortar	422	285	76,761	9.3	0.034
Both faces, 8-cal wire mesh with mortar	470	307	55,769	9.6	0.053
Single face, synthetic fiber with mortar	316	253	34,925	7.8	0.057
Single face, 8-cal wire mesh with mortar	352	291	53,524	7.6	0.041
Single face, steel fiber with mortar	320	294	40,186	6.8	0.050
Fiberglass mesh with premixed mortar	1690	232	27,669	45.6	0.38
Moderate-strength buckling-restrained brace	1994	291	264,078	42.8	0.047
High-strength buckling-restrained brace	4826	564	213,005	53.5	0.14
8-cal wire mesh with mortar and synthetic fiber	373	351	71,255	6.7	0.033
8-cal wire mesh with mortar and steel fiber	377	309	63,016	7.6	0.037

6. Conclusions

Results from rehabilitated confined masonry walls tested under reversed cyclic loading were presented from an experimental program. Thirteen specimens were tested. A total of 11 out of the 13 were tested to induce repairable damage and rehabilitated using different techniques. The other two specimens were rehabilitated in an undamaged state. Rehabilitation techniques consisted of jacketing with cement mortar reinforced with welded wire meshes of different diameters (or calibers), fiberglass mesh, synthetic fibers, steel fibers, or the addition of buckling-restrained braces. The main contribution of this paper is to show experimental results that compare different techniques aiming at a better understanding of the effectiveness of rehabilitation on damaged masonry walls. Based on the analysis of experimental data, the following conclusions can be obtained:

(1) All the rehabilitation techniques were adequate since wall strength capacity increased by an average of 84 percent, and deformation capacity tended to duplicate.
(2) The strength and lateral deformation capacity of specimens rehabilitated in an original state were 19 percent greater than those of initially damaged walls rehabilitated.
(3) Specimens rehabilitated on both faces exhibited a slide-controlled failure followed by crushing at the wall toe. This mode of failure is credited to the increase in shear strength by jacketing on both sides.
(4) The stiffness of the rehabilitated walls was consistently larger than that of the original specimens.
(5) Stiffness degraded with drift. At the start of the test, stiffness was different from that calculated using mechanical principles. The modulus of elasticity prescribed in design specifications (such as the NTC-Masonry [28]) should be revisited and modified.
(6) In the original specimens tested, residual crack widths were, on average, close to 1 mm at lateral drifts to 0.002 and 5 mm at drifts to 0.005. Crack widths in rehabilitated walls were, on average, 55% smaller than their original counterparts.
(7) As found in other experimental programs, specimens rehabilitated with welded wire meshes and cement mortar exhibited superior performance compared to the original walls. Unlike the original specimens, which presented a few large prominent inclined cracks in the wall, rehabilitated walls presented a uniform distribution of small-width cracks. In most cases, the strength and deformation capacity of walls jacketed with WWM and cement mortar were roughly double those for the original specimens.
(8) Compared to the specimen rehabilitated with fiberglass mesh, the specimens rehabilitated with steel welded wire mesh developed almost the same maximum lateral deformation. However, in terms of strength, the latter had 25% more capacity. Considering the cost, the rehabilitation with welded wire mesh was considered more adequate.
(9) Adding buckling-restrained braces is an attractive option for seismic rehabilitation, especially when weight (or mass) should be removed from the structure. Specimens exhibited wide and stable hysteresis cycles without strength degradation. Cracking in concrete tie-column and bond-beam elements contributed to stiffness degradation.
(10) The specimen with tie columns reinforced with welded-wire steel cages showed poor behavior. After rehabilitation with mortar and WWM jacketing, significant improvement in its deformation and load capacity was seen.

Similar to others, this study has limitations. For example, the out-of-plane effect was not considered when it was known that out-of-plane deformation can significantly affect the seismic performance of structures subjected to earthquakes. Additionally, only a few specimens were tested under quasi-static cyclic loading and with an aspect ratio of 1:1. Further investigations should overcome those limitations, for example, by performing more experimental tests varying the aspect ratio and considering out-of-plan deformation or other effects.

Author Contributions: Conceptualization, H.G., S.M.A. and O.L.B.; Methodology, H.G.; Investigation, C.L.; Data curation, C.L., S.M.A. and O.L.B.; Writing—original draft, C.L.; Writing—review & editing, C.L., Hector Guerrero, S.M.A. and O.L.B. All authors have read and agreed to the published version of the manuscript.

Funding: This research was funded by the Consejo Nacional de Ciencia y Tecnología (CONACyT) grant number FORDECyT 297246.

Data Availability Statement: Research data regarding this publication are available upon request to: hguerrerob@iingen.unam.mx.

Acknowledgments: The authors gratefully acknowledge the facilities provided by the National Center for Disaster Prevention (CENAPRED) and the Institute of Engineering of the National Autonomous University of Mexico (II-UNAM). Sika and Industrial Bloquera are thanked for the donation of materials and labor. We also thank Dampo Systems for donating the buckling-restrained braces used in this project.

Conflicts of Interest: The authors declare no conflict of interest.

References

1. Meli, R.; Brzev, S.; Astroza, M.; Boen, T.; Crisafulli, F.; Dai, J. *Seismic Design Guide for Low-Rise Confined Masonry Buildings*; Earthquake Engineering Research Institute (EERI): Oakland, CA, USA, 2011.
2. Marques, R.; Lourenço, P.B. Structural behavior, and design rules of confined masonry walls: Review and proposals. *Constr. Build. Mater.* **2019**, *217*, 137–155. [CrossRef]
3. Varela, J.; Fernández, L.; Gamboa, J.; Prieto, A.; Moreno, J. Flexural behavior of confined masonry walls subjected to in-plane lateral loads. *Earthq. Spectra* **2019**, *35*, 405–422. [CrossRef]
4. León, I.; Flores, L.E.; Reyes, C. Experimental study of masonry walls subjected to pure compression [CD-ROM]. In Proceedings of the XIV National Structural Engineering Congress, Acapulco, Mexico, 29–31 October 2004. (In Spanish).
5. Cao, X.; Shen, D.; Feng, D.; Wang, C.; Qu, Z.; Wu, G. Seismic retrofitting of existing frame buildings through externally attached sub-structures: State of the art review and future perspectives. *Build. Eng.* **2022**, *57*, 2352–7102. [CrossRef]
6. Bhattacharya, S.; Nayak, S.; Dutta, S.C. A critical review of retrofitting methods for unreinforced masonry structures. *Int. J. Disaster Risk Reduct.* **2014**, *7*, 51–67. [CrossRef]
7. El-Diasity, M.; Okail, H.; Kamal, O.; Said, M. Structural performance of confined masonry walls retrofitted using ferrocement and GFRP under in-plane cyclic loading. *Eng. Struct.* **2015**, *94*, 54–69. [CrossRef]
8. Gattesco, N.; Boem, I. Out-of-plane behaviour of reinforced masonry walls: Experimental and numerical study. *Compos. B* **2017**, *128*, 39–52. [CrossRef]
9. Cruz, A.; Pérez, G.J.J. Seismic performance of confined masonry walls with joint reinforcement and aspect ratio: An experimental study. *Eng. Struct.* **2021**, *242*, 112484. [CrossRef]
10. Diaz, M.; Zavala, C.; Gallardo, J.; Lavado, L. Experimental study of non-engineered confined masonry wall retrofitted with wire mesh and cement-sand mortar. In Proceedings of the 16th Conference on Earthquake Engineering, Santiago, Chile, 9–13 January 2017.
11. Shermi, C.; Dubey, R.N. Study on out-of-plane behaviour of unreinforced masonry strengthened with welded wire mesh and mortar. *Constr. Build. Mater.* **2017**, *143*, 104–120. [CrossRef]
12. Alcocer, S.M.; Pineda, J.A.; Ruiz, J.; Zepeda, J.A. Retrofitting of Confined Masonry Walls with Welded Wire Mesh. In Proceedings of the 11th Word Conference on Earthquake Engineering, Acapulco, Mexico, 23–28 June 1996; Elsevier: Amsterdam, The Netherlands, 1996. Article No. 1471.
13. Alcocer, S.M. Use of horizontal steel and wire mesh as strengthening options for confined masonry walls. In Proceedings of the 7th Chilean Conference on Seismology and Earthquake Engineering and First Iberoamericano Earthquake Engineering Congress, La Serena, Chile, 9–13 November 1997; Volume 1, pp. 195–204. (In Spanish).
14. SMIE. *Masonry Buildings*; Mexican Society of Structural Engineering: Mexico City, Mexico, 2019. (In Spanish)
15. Can, Ö. Investigation of seismic performance of in-plane aligned masonry panels strengthened with Carbon Fiber Reinforced Polymer. *Constr. Build. Mater.* **2018**, *186*, 854–862. [CrossRef]
16. D'Ambra, C.; Lignola, G.P.; Prota, A.; Sacco, E.; Fabbrocino, F. Experimental performance of FRCM retrofit on out-of-plane behaviour of clay bricks walls. *Compos. B* **2018**, *148*, 198–206. [CrossRef]
17. Martins, A.; Vasconcelos, G.; Fangueiro, R.; Cunha, F. Experimental assessment of an innovative strengthening material for brick masonry infills. *Compos. B Eng.* **2015**, *80*, 328–342. [CrossRef]
18. Ghiassi, B.; Oliveira, D.V.; Marques, V.; Soares, E.; Maljaee, H. Multi-level characterization of steel reinforced mortars for strengthening of masonry structures. *Mater. Des.* **2016**, *110*, 903–913. [CrossRef]
19. Yacila, J.; Salsavilca, J.; Tarque, N.; Camata, G. Experimental assessment of confined masonry walls retrofitted with SRG under lateral cyclic loads. *Eng. Struct.* **2019**, *199*, 109555. [CrossRef]

20. Deng, M.; Yang, S. Experimental and numerical evaluation of confined masonry walls retrofitted with engineered cementitious composites. *Eng. Struct.* **2020**, *207*, 110249. [CrossRef]
21. Deng, M.; Zhang, W.; Yang, S. In-plane seismic behavior of autoclaved aerated concrete block masonry walls retrofitted with high ductile fiber-reinforced concrete. *Eng. Struct.* **2020**, *219*, 110854. [CrossRef]
22. JICA—Japan International Cooperation Agency. National Center for Disaster Prevention (CENAPRED). February 2020. Available online: https://www.jica.go.jp/mexico/espanol/activities/disaster_01.html (accessed on 1 January 2023).
23. Sika MonoTop—722 Mur. One-Component Mortar for the Repair and Strengthening of Traditional Walls. In *Technical Sheet*; Sika: Mexico City, Mexico, 2020. (In Spanish)
24. Sika Fiber Force PP-48. Macro Synthetic Fibers for Strengthening of Concrete and Mortar. In *Technical Sheet*; Sika: Mexico City, Mexico, 2019. (In Spanish)
25. Sika Fiber Xorex. Steel Fiber for Concrete and Mortar Strengthening. In *Technical Sheet*; Sika: Mexico City, Mexico, 2020. (In Spanish)
26. StoneCrete. Mortar for structural covering. In *Technical Sheet*; Industrial Mexicana S.A. de C.V.: Mexico City, Mexico, 2018. (In Spanish)
27. *ASTM C39/C39M-12*; Standard Test Method for Compressive Strength of Cylindrical Concrete Specimens. ASTM International: West Conshohocken, PA, USA, 2012.
28. NTC-Masonry. *Complementary Technical Standards for the Design and Construction of Masonry Structures*; Official Gazette of Mexico City, Government of Mexico City: Mexico City, Mexico, 2020. (In Spanish)
29. *ASTM C469/C469M-10*; Standard Test Method for Static Modulus of Elasticity and Poisson's Ratio of Concrete in Compression. ASTM International: West Conshohocken, PA, USA, 2010.
30. *NMX-C-464-ONNCCE*; Construction Industry—Masonry—Determination of Diagonal Compressive Strength and Shear Modulus of Prisms, As Well As Determination of Compressive Strength and Elastic Modulus of Clay or Concrete Masonry Prism—Test Method, Mexican Standards. National Agency for Standardization and Certification of Construction and Building: Mexico City, Mexico, 2010. (In Spanish)
31. *ASTM E519-15*; Standard Test Method for Diagonal Tension (Shear) in Masonry Assemblages. ASTM International: West Conshohocken, PA, USA, 2015.
32. Cao, X.; Xiong, C.; Feng, D.; Wu, G. Dynamic and probabilistic seismic performance assessment of precast prestressed reinforced concrete frames incorporating slab influence through three-dimensional spatial model. *Bull. Earthq. Eng.* **2022**, *20*, 6705–6739. [CrossRef]
33. Aloisio, A.; Contento, A.; Alaggio, R.; Briseghella, B.; Fragiacomo, M. Probabilistic Assessment of a light-timber frame shear wall with variable pinching under repeated earthquakes. *Struct. Eng.* **2022**, *148*, 04022178. [CrossRef]
34. *FEMA P-356*; Prestandard and Commentary for the Seismic Rehabilitation of Buildings. Federal Emergency Management Agency: Washington, DC, USA, 2000.
35. *FEMA P-795*; Quantification of Building Seismic Performance Factors: Component Equivalency Methodology. Federal Emergency Management Agency: Washington, DC, USA, 2011.
36. NTC-Seismic. *Complementary Technical Standards for Seismic Design*; Official Gazette of Mexico City, Government of Mexico City: Mexico City, Mexico, 2020. (In Spanish)
37. Lubin, C. Experimental Behavior of Masonry Walls Rehabilitated with Different Techniques Subjected to Cyclic Loading. Master's Dissertation, National Autonomous University of Mexico, Ciudad Universitaria, Mexico City, Mexico, 2022. (In Spanish).